

Improvement of RTK-GNSS with Low-Cost Sensors Based on Accurate Vehicle Motion Estimation Using GNSS Doppler

Aoki Takanose, Kanamu Takikawa, Takuya Arakawa, and Junichi Meguro

Abstract— This study proposes a method for estimating the positions of vehicles in urban environments with high accuracy. We employ satellite positioning by GNSS for position estimation. Real-time kinematic-global navigation satellite systems (RTK-GNSS) with high precision in satellite positioning can estimate positions with centimeter-scale accuracy. However, in urban areas, the position estimation performance deteriorates owing to multipath errors. Therefore, we propose a method to improve the positioning results by increasing the robustness against multipath using vehicle trajectory. The vehicle trajectory estimates the travel route using the attitude angle and speed. Attitude angles are heading, pitching and slip angle. Trajectories can be generated with 0.5m error performance per 100m. In the proposed method, the trajectory is used as a constraint to solve the multipath of RTK-GNSS. In the evaluation test, the ratio of high-accuracy position estimation improved by up to approximately 30% compared to the conventional method. It is assumed that this method can enhance the development of self-driving cars, AGV control and SLAM technology by eliminating errors and calculating reliability.

I. INTRODUCTION

GNSS positioning is widely used in various applications and, in appropriate environments, the RTK-GNSS can estimate position with centimeter-scale accuracy [1]. In recent years, active use in autonomous vehicles has been conspicuous. Autonomous vehicles require high-precision position results [2-3]. RTK-GNSS is used not only for self-driving vehicles, but also for integration of transport robots such as AGVs and SLAM technology [4-6]. It is also used as a reference to evaluate position estimation results obtained with SLAM and other technologies [7-8].

However, RTK-GNSS does not always provide high accuracy. In urban areas, multipath occurs when radio waves are reflected and diffracted. Satellite positioning is vulnerable to multipath. Multipath is one of the more difficult problems to solve for satellite positioning.

We improve robustness against multipath at low cost. We can estimate the exact trajectory from the posture and speed of the moving object [9]. The trajectory from which multipath have been eliminated can be estimated with 0.5m performance per 100m. In the proposed method, the trajectory is integrated at the point where the robustness of the conventional method is largely lacking. This integration is not just an integration like tightly coupled or loosely coupled. Basically, the conventional RTK-GNSS framework is used. However, optimization is performed using the trajectory as

the initial condition of the FLOAT solution necessary for searching for the FIX solution. This is a new method that uses the trajectory as the initial condition, and the improved robustness with the trajectory improves the final position estimation result.

II. RELATED WORKS

RTK-GNSS is a technique used to estimate the position of objects with centimeter-scale accuracy. First, the FLOAT solutions are estimated with a Kalman filter. Then, the integer ambiguities are resolved using the least squares ambiguity decorrelation (LAMBDA) [10] and Ratio-Test [1] methods. Finally, the FIX solutions, which are highly accurate position results, are calculated using the resolved ambiguities. However, the RTK-GNSS sometimes fails to calculate positions in urban areas. The main cause is a multipath error.

Various methods have been proposed to solve this problem. The method of integrating IMU is effective for improving the utilization rate of location estimation [11-12]. Even when satellites cannot be observed, they are often used because position estimation is possible. Gaussian filters are often used for integration. However, since the multipath error has a non-normal distribution, the filter may diverge. Even so, errors tend to increase due to the bias of the IMU. For IMUs, there are solutions that use expensive ones, such as Fiber Optic Gyros (FOG). However, multipath will continue to affect you unless you remove it.

On the other hand, there is also a method that uses a camera or 3D LIDAR to remove multipath signals [13-14]. When receiving a signal that has received multipath, it may receive satellite radio waves that are not directly visible due to obstructions. This is called Non Line Of Sight (NLOS). In order to eliminate NLOS, satellites are identified using a zenith camera or 3D LIDAR. However, the judgment requires an accurate posture and a high-precision 3D map.

There is also a method that focuses on RTK algorithms [15-16]. It is known that it is difficult to obtain a FIX solution in a multipath environment. The major issue here is integer ambiguity due to poor FLOAT solutions. The FLOAT solutions are calculated by the Kalman filter, which uses single positioning results as initial values. The Kalman filter outputs suitable results if the errors in the single positioning results exhibit a normal distribution. However, the single positioning in urban areas suffers from errors of several tens of meters or more, and the distribution is non-normal. The FIX solution is estimated based on the FLOAT solution.

Aoki Takanose master course student of the Division of Mechatronics Engineering, Graduate School of Science and Technology, Meijo University, Shiogamaguti 1-501, Tenpaku-ku, Nagoya, Aichi
(193432009@cmailg.meijo-u.ac.jp)

Takuya Arakawa and Kanamu Takikawa are master course students of the Division of Mechatronics Engineering, Graduate School of Science and

Technology, Meijo University. (183432001 / 193432010@cmailg.meijo-u.ac.jp)

Junichi Meguro is an Associate Professor with the Department of Mechatronics Engineering, Faculty of Science and Technology, Meijo University. (e-mail: meguro@meijo-u.ac.jp).

Therefore, incorrect FLOAT solutions derived from non-normally distributed single position results lead to incorrect FIX solutions in the LAMBDA method (Figure 1).

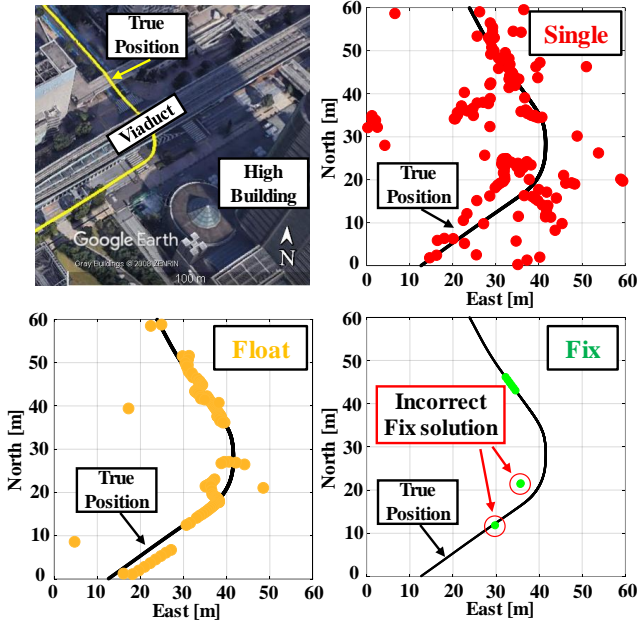


Figure 1 Large errors with multipath in urban area

A method that improves the initial condition of the Kalman filter to estimate the FLOAT solution has been proposed [16]. This method uses the previous FIX solution and GNSS Doppler methods. According to Shimizu, the method improved the accuracy of the determination of integer ambiguity and confirmed the improvement of the availability rate. However, in urban areas, the FIX solutions and velocity vectors calculated by GNSS Doppler are also affected by multipath errors. Therefore, FIX solutions are occasionally inaccurate because the accuracy of the predicted values for the Kalman filter is decreased. In order to improve the accuracy of RTK-GNSS in urban areas, it is necessary for this prediction to have high accuracy and the error to be close to normal distribution.

III. OUR PROPOSAL

In this paper, we propose a new technique that improves the accuracy of the RTK-GNSS in urban areas. Figure 2 shows an overview of our approach. This method is roughly divided into two domains. One is the trajectory estimation domain that integrates GNSS and IMU (inertial measurement unit) and improves robustness [9]. Trajectory is estimated from the attitude angle and the wheel speed. Trajectory improves performance by making use of the features of GNSS Doppler. GNSS Doppler has the feature that error mean is zero. However, accuracy is degraded due to multipath. Therefore, the performance can be improved by judging and averaging the GNSS Doppler error with the IMU. The trajectory enables accurate and robust estimation of relative and absolute positions. This system exhibits a relative positional accuracy of 0.5 m per 100 m and an absolute positional accuracy of 1.5

m in urban environments. The technology required for trajectory estimation will be described later.

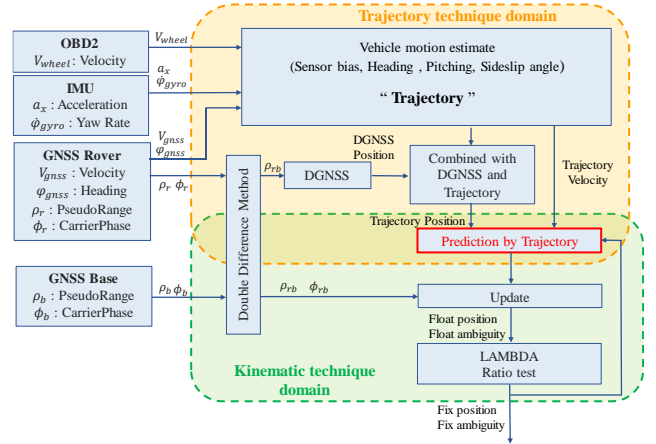


Figure 2 Flowchart of the proposed method

The other domain is the kinematic technique domain that has been used in the past. Conventionally, the prediction step in this domain has lacked robustness. In general, RTK-GNSS, a Kalman filter is used for FLOAT solution estimation. The one-step state transition and measurement equation for the Kalman filter can be described as follows:

$$\mathbf{X}_{k+1} = \mathbf{F}_{k,k+1}\mathbf{X}_k + \mathbf{W}_k \quad (1)$$

$$\mathbf{Z}_{k+1} = [\boldsymbol{\phi}_{rb}^T, \boldsymbol{\rho}_{rb}^T]^T = \mathbf{h}(\mathbf{X}_{k+1}) + \mathbf{V}_{k+1} \quad (2)$$

where \mathbf{F} is a one-step transition matrix, \mathbf{Z} is an observation variable of carrier phase $\boldsymbol{\phi}$ and pseudorange $\boldsymbol{\rho}$, and \mathbf{W} and \mathbf{V} are system noise and observation noise. Since the observation equation is nonlinear, an extended Kalman filter is used. The state variables are as follows:

$$\mathbf{X} = [\mathbf{r}_{est}^T, \mathbf{N}^T]^T \quad (3)$$

where \mathbf{r}_{est} is the receiver position and \mathbf{N} is the ambiguity of each satellite. Note that the ambiguity is the number of satellites observed, and the estimated value is a real value. The integer value of the ambiguity is searched using the value obtained here. Therefore, this step is very important process to improve the accuracy of the subsequent stage.

In the method of reference [1], a single positioning solution is used without using the previous estimated position at the time of state transition. Since the individual positioning solution is used in each epoch, it can be said that the initial conditions for estimating the FLOAT solution are updated each time. Therefore, the state transition equations can be rewritten as:

$$\mathbf{X}_{k+1} = \mathbf{F}_{k,k+1}\mathbf{X}_k + \mathbf{X}_{init_k} + \mathbf{W}_k \quad (4)$$

$$\mathbf{F}_{k,k+1} = \text{diag}[\mathbf{0}, \mathbf{I}], \quad \mathbf{X}_{init_k} = [\mathbf{r}_{single}^T, \mathbf{0}]^T \quad (5)$$

where \mathbf{X}_{init} is the initial value, and the method from [1] is a single positioning solution. However, as shown in the previous section (Figure 1), the single positioning solution is subject to multipath and non-normally errors in urban areas. When single positioning is used, the accuracy of the predicted value is low, and the error remains non-normally distributed. Therefore, in the final result, the position is estimated with large errors.

Our method introduces a trajectory to this prediction step. The proposed method improves this step by reducing non-normal distribution errors in initial values and adding robustness. The trajectory is integrated and estimated so that the error mean becomes zero. Therefore, the trajectory error is very close to the normal distribution. We think that the trajectory can be applied to the Kalman filter. In addition, since the accuracy of the trajectory is high, improvement of the estimation accuracy of the FLOAT solution can be expected. At first, it changes the initial positioning solution, which is a single positioning solution, to the estimated position \mathbf{B} that combines trajectory and GNSS. \mathbf{B} is a robust location result that rejects multipath. Accuracy is sub-meter class. The state transition is as follows:

$$\mathbf{F}_{k,k+1} = \text{diag}[\mathbf{0}, \mathbf{I}], \quad \mathbf{X}_{init_k} = [\mathbf{B}^T, \mathbf{0}]^T \quad (6)$$

The position estimation that combines the trajectory and GNSS is close to a normal distribution by averaging out the errors.

In the LAMBDA method, it is effective to search for ambiguity more accurately by limiting the range. The method in reference [16] uses the FIX solution from the previous step, and the velocity vector obtained from GNSS Doppler, to limit the search range (Figure 3). Using the prior method [16], the percentage of FIX solutions obtained increases. However, in urban areas, there are few FIX solutions and GNSS Doppler also experiences multipath. In the proposed method, the trajectory of the motion vector of the vehicle is used instead of the GNSS Doppler. By changing to the trajectory, improvement in robustness against multipath can be expected. In this case, the state transition equation is as shown below.

$$\mathbf{F}_{k,k+1} = \mathbf{I}, \quad \mathbf{X}_{init_k} = [\mathbf{V}^T \cdot dt, \mathbf{0}]^T \quad (7)$$

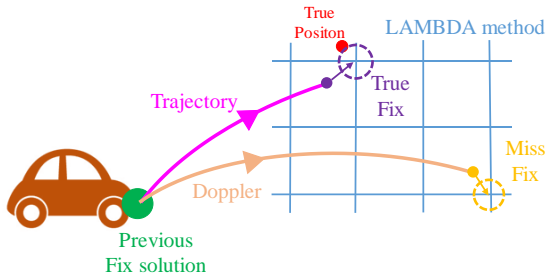


Figure 3 Predicted position estimation by FIX solution and 3D Trajectory

IV. TRAJECTORY TECHNIQUE DOMAIN

A. Trajectory estimation considering vehicle motion

The trajectory estimation, which is the core of the proposed method, is explained below. This is one of the methods to integrate GNSS and IMU [17-19]. Gaussian filters are often used for GNSS and IMU integration. The error can be reduced by using Gauss Filter. However, estimation is likely to fail in an environment where multipath occur frequently [20-21]. That is because the error noise has a non-normal distribution. Therefore, we estimate while removing multipath. Estimate by accumulating data for a long time instead of sequential estimation like Gaussian filter. This is the biggest feature of our method. Also, overall optimization such as estimating the attitude angle and vehicle speed at the same time is not

performed. Estimates are carefully made one by one using a combination of compatible data. This time, in addition to the azimuth and pitch angles estimated in reference [9], add the error of wheel speed and slip angle. In addition, the technology required for the proposed method will be explained.

B. Wheel speedometer error estimation

Wheel speedometer is calculated from the number of revolutions of the driveshaft and the tire diameter. However, the wheel speed includes an error due to the ratio of the actual tire diameter to the reference. Here, it is assumed that the correction for the ratio of the tire diameter, which is the dominant error factor, relies on the scale factor SF related to the original speed. The actual velocity \bar{V} with respect to the measured wheel speed V_{wheel} is expressed as in Equation (8).

$$\bar{V} = V_{\text{wheel}} \cdot SF \quad (8)$$

However, GNSS Doppler measurements can estimate velocity V_{gnss} [22] very accurately in environments with good satellite signals. Therefore, V_{gnss} can be regarded as the actual velocity \bar{V} in a good environment. Under that assumption, SF can be calculated with Equation (9).

$$SF(t) = \frac{V_{\text{gnss}}(t)}{V_{\text{wheel}}(t)} \quad (9)$$

However, V_{gnss} is not always accurate. As it is, SF rarely fluctuates dynamically, so it is often acceptable to use the estimated value continuously. Therefore, the proposed method only accumulates data in good environments and uses the average value as SF .

C. Heading angle and Yaw rate error estimation

The heading angle is estimated by combining GNSS Doppler and yaw rate. The GNSS Doppler can use satellite data to obtain the heading angle relative to the north reference from the velocity vector and the relative velocity (Figure 4).

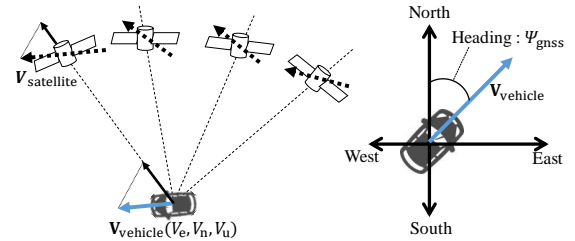


Figure 4 The image of Heading estimation with Doppler

The proposed heading angle estimation is integrated as follows:

$$\Psi_{\text{gyro}} = \Psi_{\text{init}} - \int_{t-k}^t \dot{\phi} dt \quad (10)$$

$$\Psi_{\text{init}} = \text{argmin} \sum (\Psi_{\text{gnss}} - \Psi_{\text{gyro}})^2 \quad (11)$$

where Ψ_{gnss} is the heading angle obtained from GNSS Doppler, Ψ_{gyro} is the relative heading angle accumulated

from the yaw rate of the gyro, and $\dot{\Psi}$ is the yaw rate. For integration, data for the prior 30 seconds are used. The heading angle is the result calculated by the minimization of Equation (11) for the 30 second intervals. After that, the heading angle is calculated by integrating the yaw rate from Ψ_{init} . The heading angle by GNSS Doppler has an error due to the influence of multipath in urban areas [22]. As a result, Ψ_{init} has a large error when it receives multipath from GNSS. In the proposed method, if the residual between the accumulated Ψ_{gyro} and the time series Ψ_{gnss} is large, it is determined that GNSS has experienced multipath and the data are eliminated (Figure 5). With this process, bad data are rejected and the optimal Ψ_{init} can be estimated.

Our method is characterized by the use of data from a long time series, and it is difficult to distinguish GNSS multipath in a short time. This feature is essential for improving the heading angle accuracy relative to that obtained with the conventional method.

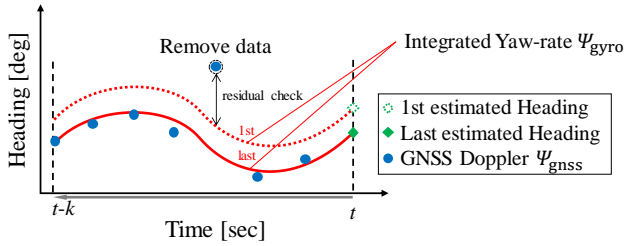


Figure 5 Heading angle estimation

On the other hand, the yaw rate obtained from the IMU includes an error. If uncorrected long-term data are used, the calculation may fail. Therefore, the yaw rate error must be corrected. Yaw rate error is caused by the offset of the IMU bias. This offset amount can be approximated from the difference between the integration of yaw rate over a long time period (several minutes) and Ψ_{init} (Figure 6). Therefore, yaw rate error is also estimated with the result of heading estimation. Estimation of the yaw rate error allows long-time use of yaw rate. In addition, even when GNSS cannot be received, the heading angle can be estimated by connecting at the yaw rate.

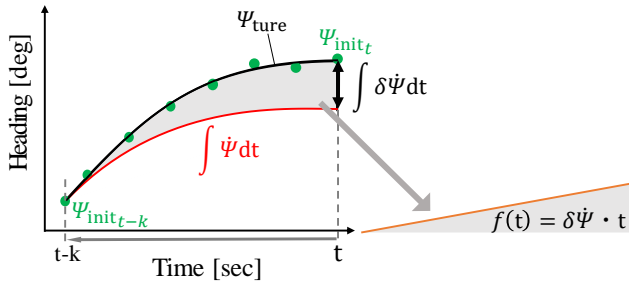


Figure 6 Yaw rate offset estimation

D. Side slip angle estimation

When a vehicle turns, there is a difference between the direction it is facing and the direction in which it is moving. This difference is called the sideslip angle. What can be measured from the IMU is the direction in which the vehicle faces. But what one really needs is the direction in which it is moving. This angle plays an important role in heading angle

estimation and it is, therefore, necessary to determine the sideslip angle. In the conventional method [23,24], an observer is established and the parameters necessary for estimating the sideslip angle are measured. However, it is difficult to measure everything accurately.

We utilize a simple model to estimate the sideslip angle and it uses a two-wheel vehicle model for simplicity. According to the two-wheel vehicle model, the sideslip angle β can be expressed as:

$$\beta = -\frac{mL_f}{2LK_r}\dot{\Psi}V \quad (12)$$

where m is the mass of the vehicle, K_r is the cornering power of the rear wheels, V is the speed of the center of gravity, L_f is the distance between the front wheel axle and the vehicle's center of gravity, and L is the distance between the front wheel axle and the rear wheel axle. Even when using a two-wheel model, these parameters are required to determine the sideslip angle.

Here, we recall that the GNSS Doppler measurement is the relative speed of the satellite and the receiver. In other words, the heading angle obtained from GNSS Doppler indicates the direction in which the vehicle is moving. When the vehicle is in a curve, the difference between the GNSS Doppler heading angle and the yaw rate accumulation heading angle is the sideslip angle. (see Figure 7 and Equation 13).

$$\beta = \Psi_{gyro} - \Psi_{gnss} \quad (13)$$

Most of the parameters in Equation (12) are vehicle-specific parameters. We define the coefficient K such that:

$$K = -\frac{mL_f}{2LK_r} \quad (14)$$

If K can be determined, the sideslip angle can be determined in the two-wheel model. Using Equation (12-14), the coefficient K is substituted as follows:

$$\beta = \Psi_{gyro} - \Psi_{gnss} = K\dot{\Psi}V \quad (15)$$

The coefficient K can then be determined from Equation (15):

$$K = \frac{\Psi_{gyro} - \Psi_{gnss}}{\dot{\Psi}V} \quad (16)$$

However, the right side of Equation (16) contains an error. In our method, the coefficient K is determined using the least squares method. By calculating the coefficient K , the sideslip angle can be calculated accurately even when GNSS cannot be received.

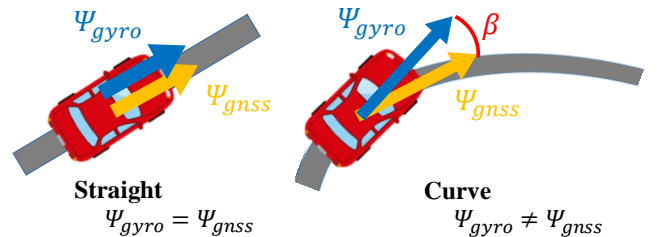


Figure 7 The image of Sideslip angle estimate

E. Positioning with combining Trajectory and GNSS

Sections B to D describe methods for estimating each element of vehicle motions. The pitch angle φ is estimated based on the method [9]. The velocity vector based on vehicle motions can be calculated as follows:

$$\mathbf{V} = SF \cdot V_{\text{wheel}} \cdot \mathbf{R}(\Psi + \beta, \varphi) \quad (17)$$

where $\mathbf{R}(\Psi + \beta, \varphi)$ is the attitude angle vector. At present, the roll angle is not estimated. It is assumed that the roll angle is not a factor on ordinary roads, so the roll angle is taken to be 0. In this paper, the trajectory is defined as this velocity vector, or the relative position variation that can be obtained by accumulating it. The trajectory can thus be accurately generated for the actual route (Figure 8).

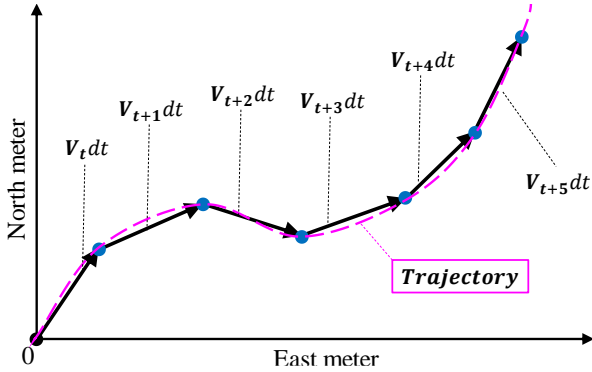


Figure 8 Overview of calculate trajectory

In the proposed method, since the shape of the trajectory is accurate, the current position is estimated using the shape as a constraint. This position estimation algorithm is applied in the same way as is the heading angle. The position estimation based on the trajectory and the GNSS position is estimated with the following equations:

$$\mathbf{T} = \mathbf{B} - \int_{t-k}^t \mathbf{V} \cdot dt \quad (18)$$

$$\mathbf{B} = \text{argmin} \sum (\mathbf{P} - \mathbf{T})^2 \quad (19)$$

where \mathbf{P} is the GNSS position, \mathbf{T} is the trajectory positions, \mathbf{V} is the vehicle velocity vector, and \mathbf{B} is the estimated position. The running trajectory is generated by integrating the vehicle velocity vector resulting from any \mathbf{B}_{init} . The trajectory is combined with the GNSS position result using the least-squares method. The GNSS position results are compared with the trajectory, and the positioning results when large residuals are removed. Again, the trajectory and the GNSS positioning result are combined, and the estimated position is again estimated. This is repeated until the maximum value of the residuals falls below the threshold, indicating that the rejection of the bad GNSS positioning result has been completed, and the result is the estimated position. It is obvious that the robustness is improved by removing the satellites that have received multipath signals.

V. PREDICTION OPTIMIZATION AND UPDATES

As shown in Chapter 3, the FLOAT solution is estimated by a Kalman filter. In the prediction step, they are shown by

equations (1-4) and (5,6). At present, there are two prediction steps. In the LABMDA method, the performance improves as the search range is further limited. Therefore, a method with high estimation accuracy that can limit the search range should be selected. Equation (6) is considered to be more accurate than Equation (5) because the FIX solution is used. Therefore, when a FIX solution is obtained, the prediction is updated using equation (6). In other cases, equation (5) is used. In the proposed method, optimization is performed by switching predictions. This switch is important and plays a role in keeping the LAMBDA method with accurate estimates. As a result, the robustness can be improved using the trajectory, and highly accurate estimation can be performed.

Following the prediction step is the observation step. The observation step is performed in the same way as the conventional method [1].

VI. EVALUATION TESTS

A. Outline of evaluation testing

We evaluated our proposed method and conventional techniques using sensor data collected in the urban areas of Tokyo, Japan. We performed the evaluation using two locations. The first route (Route A) is a standard urban area with many buildings and viaducts. The second route (Route B) is a dense urban area surrounded by high-rise buildings. Table 1 shows the list of sensors used for the evaluation test. The GNSS receiver is a Ublox F9P that can receive GPS, BeiDou, and QZSS signals of 5 Hz frequency. Ublox F9P is the standard GNSS receiver for automobiles. In addition, we use automotive level MEMS-IMU. Table 2 shows the evaluation methods. Figure 9 shows the appearance of the equipment used in the experiment.

Table 1 Equipment used for evaluation

Equipment	Manufacturer	Model(cycle)
GNSS antenna	Trimble	Zephyr model 3
GNSS receiver	Ublox	F9P (5Hz)
IMU	Tamagawa Seiki	TAG264 (50Hz)
Reference	Applanix	POSLV 620

Table 2 List of evaluation methods

Name	Define
Method [1]	Method 1
Method [16]	Method 2
DGNSS & Trajectory[9]	Method 3
Proposed method	Proposal



Figure 9 Experimental car exterior

B. Evaluation test in Urban Area (Route A)

Figure 10 shows the route around Route A and Figure 11 shows the number of observation satellites.

Figure 12 shows the positioning results obtained with the conventional methods 1 and 2 and with the proposed method, and it indicates whether each method is a FLOAT solution or a FIX solution. The percentage of FIX solutions obtained is shown next to the legend. This designated location has a shopping mall on the south side, under a railway overpass. Even in such a multipath environment, the ratio of FIX solutions obtained by the proposed method is higher than that of the conventional methods.

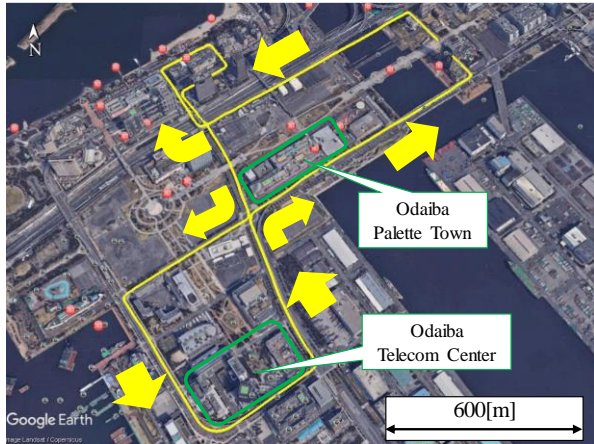


Figure 10 Evaluation route in Route A (5.8km)

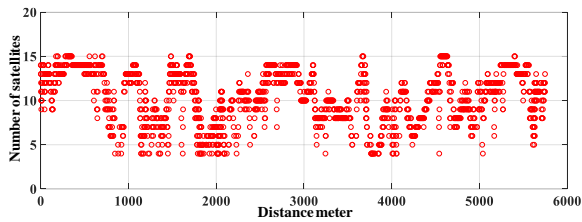


Figure 11 Number of satellites used in Route A

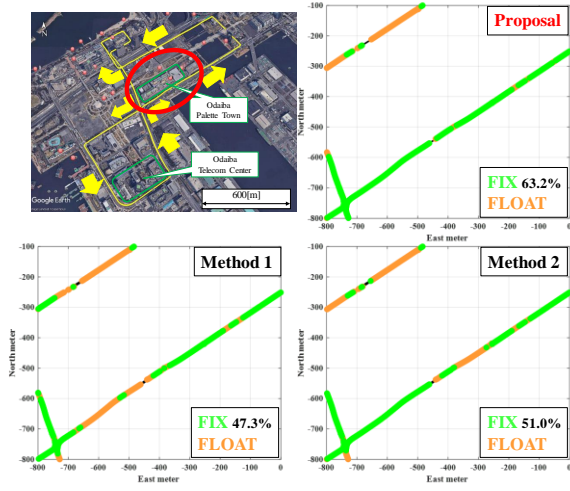


Figure 12 Part of the position result 1

In Figure 13, the results from each method and the true values are displayed for a situation involving waiting for a signal beside a pedestrian bridge. In conventional method 1,

it can be confirmed that the value deviates greatly from the true value. However, in the proposed method, positioning exhibits accuracy higher than that seen for the other methods.

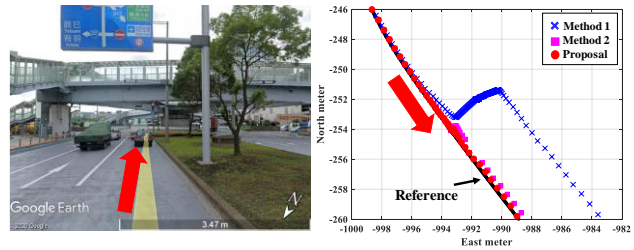


Figure 13 Each method VS Reference 1

In addition, the error is evaluated statistically. The error is the difference between the position results of each method and the reference. The evaluation is shown by the cumulative frequency distribution of the error. Figure 14 shows the evaluation results of each method.

As shown in Figure 14, Method 3 achieved lane-level accuracy (1.5 m). The achievement rate for errors within 1.5 m is 93%. However, the rate for high accuracy (errors less than 0.3 m) is lower than that of the general RTK-GNSS. On the other hand, Method 2 had a higher positioning accuracy than did the conventional RTK-GNSS. However, the amount of improvement is small (less than 5%), because the GNSS Doppler method is also affected by multipath errors. On the other hand, our proposed method improves the 1.5 m (lane-level) and 30 cm positioning accuracies simultaneously. Our proposed method integrates the advantages of Methods 1 and 2.

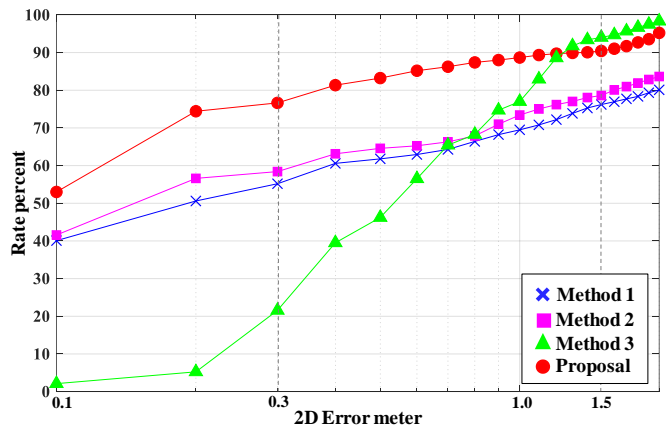


Figure 14 2D Position error rate of each method

C. Evaluation test in dense urban area

Figure 15 shows the route around Route B, which is a typical dense urban canyon surrounded by high-rise buildings. Figure 16 shows the number of observation satellites.

In route B, the performance of the trajectory is also evaluated. First, the initial position of the trajectory is adjusted to the reference. Then, integrate 100m and calculate the error from the reference. This is performed every 10m, and each error is evaluated by the cumulative frequency distribution. Figure 17 shows the trajectory evaluation.

IMU_RAW in Figure 17 is the performance of IMU without correction. Uncorrected IMU results in poor performance. On the other hand, the trajectory achieved about 90% and the error was within 0.5m. This is because the IMU is corrected and integrated with the GNSS Doppler to eliminate multipath.

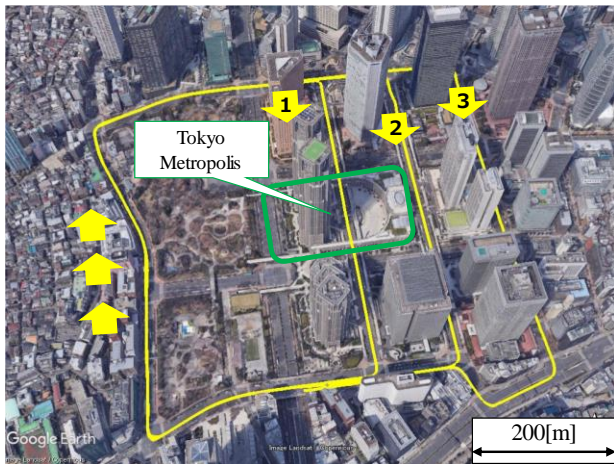


Figure 15 Evaluation route in Route B (6.6km)

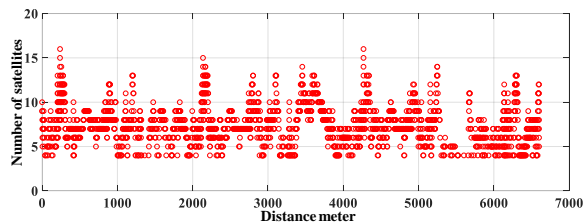


Figure 16 Number of satellites used in Route B

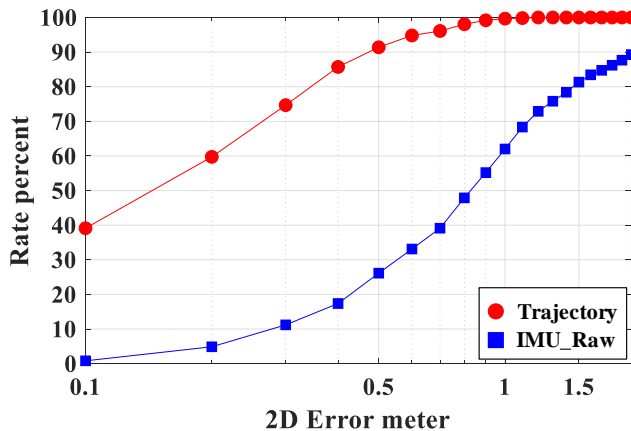


Figure 17 Evaluate of Trajectory Performance

Figure 18 shows the position estimation results for each method and the state of the solution at the specified location. In this area, buildings over 100 m lined the streets. It is a place in which multipath error is very likely to occur and accurate satellite positioning is difficult. In Methods 1 and 2, the positioning solution deviates greatly from the actual route. Also, even FIX solutions with high-reliability result in many incorrect results. In the proposed method, such errors are considerably reduced, but they do remain. Figure 19 shows the estimation result in other locations. Here the buildings line up along the west side of the street, and it can be noted that

this is also subject to multipath conditions. At this point, there is no noticeable outlier, as shown in Figure 19. However, with the conventional method, estimated values are very different from the true values. On the other hand, in the proposed method, estimated values are close to the true values.

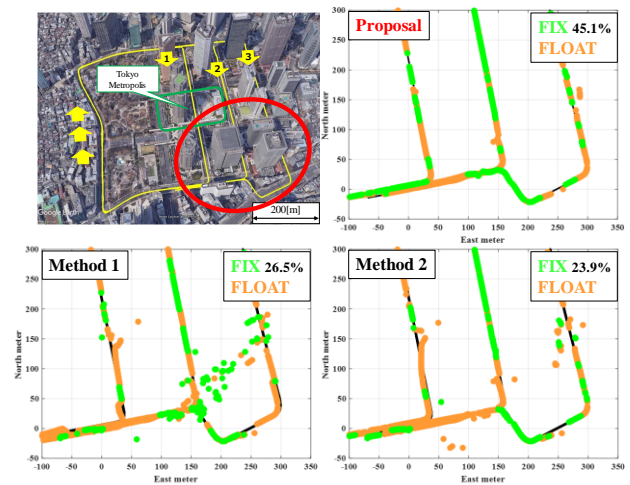


Figure 18 Part of the position result 2

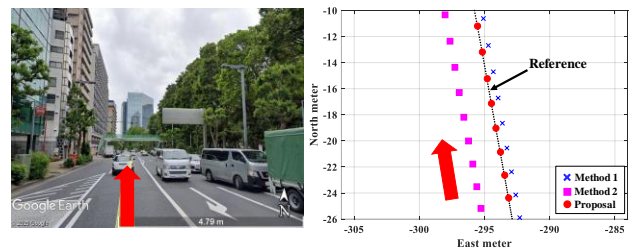


Figure 19 Each method VS Reference 2

This course was also evaluated statistically and Figure 20 shows the 2D positioning accuracy.

From Figure 20, it can be seen that the proposed method also improves the 1.5 m (lane-level) and 30 cm positioning accuracies simultaneously. Figure 20 shows that the proposed method provides more accurate positioning results in dense urban areas than do conventional techniques. On the other hand, the rate of large errors (more than 1.0 m) is increased compared to the evaluation of Route A (standard urban area)

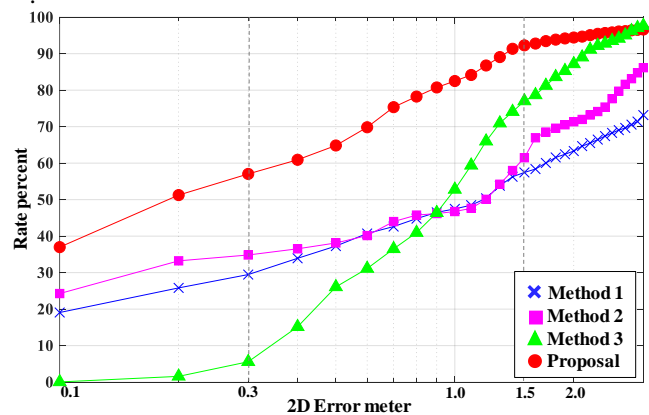


Figure 20 2D Position error rate of each method

VII. CONCUSSION

The RTK-GNSS experiences errors when it solves the integer ambiguity with multipath conditions in urban areas. This was due to the poor accuracy of the FLOAT solution required for the LAMBDA method, which estimates the FIX solution. Therefore, in this research, we proposed a method to improve the estimation accuracy of FLOAT solutions using highly accurate vehicle trajectories to suppress the effects of multipath. The biggest feature of this method is that the trajectory can be estimated with high accuracy. The trajectory is applied because the prediction step is weak against multipath. The prediction step can obtain a high prediction value by constraining it with the trajectory. Also, the trajectory is very effective for Kalman filter prediction because the noise is close to normal distribution. In the prediction step, robustness and accuracy are improved, and a highly accurate FIX solution can be obtained.

In the evaluation test, it was confirmed that the performance was higher than before. In standard urban areas, FIX is up to 15% better than other methods. In addition, the result of high-accuracy position estimation (error within 0.3m) has been improved by 25%. The results confirm that accuracy in the prediction step is important. The same goes for dense urban areas. The FIX rate has been improved by up to 20%, and the error rate within 0.3m has been improved by 30%. We believe that the proposed RTK-GNSS will enhance the development of applications such as autonomous vehicles, AGV, and SLAM technologies that require highly accurate position estimation. However, in this case, it is necessary to improve the reliability or reduce the error by combining other sensors.

Accuracy in dense urban area is degraded compared to standard urban areas. This is attributed to the observation update that has not been changed. No multipath countermeasures have been taken for observations. As a result, errors remain in dense urban areas where multipath occur frequently. We plan to improve this observable. We will make the best use of the trajectory in this plan as well.

ACKNOWLEDGEMENT

This study was conducted in the Cabinet Office's "Strategic Innovation Creation Program (SIP) Phase 2 / Autonomous Driving (System and Service Expansion) / Recognition Technology Necessary for Autonomous Driving Technology (Levels 3 and 4)." The project was commissioned by the New Energy and Industrial Technology Development Organization (NEDO).

REFERENCES

- [1] Tomoji Takasu and Akio Yasuda, "Development of the low cost RTK-GPS receiver with an open source prgram package RTKLIB. In Proceeding of the International Symposium on GPS/GNSS", Jeju, Korea, 4-6 November 2009.
- [2] Anweshan Das, Gijs Dubbelman, "An Experimental Study on Relative and Absolute Pose Graph Fusion for Vehicle Localization", IEEE IV 2018
- [3] Erik Karlsson, Nasser Mohammadiha, "A Statistical GPS Error Model for Autonomous Driving", IEEE IV 2018
- [4] Benjamin C. Heinrich, Dennis Fassbender, Hans-Joachim Wuensche, "Precise Object-Relative Positioning for Car-Like Robots", IEEE ITSC 2016
- [5] Liu Jiang, Cai Bai-gen, Wang Jian, "Track-constrained GNSS/Odometer-based Train Localization using a Particle Filter", IEEE IV 2016
- [6] Jiali Bao, Yanlei Gu, Shunsuke Kamijo, " Vehicle positioning with the integration of scene understanding and 3D map in urban environment", IEEE IV 2017
- [7] Farouk Ghallabi, Ghayath EL-HAJ-SHHADE, Marie-Anne MITTET, Fawzi Nashashibi, "LIDAR-Based road signs detection For Vehicle Localization in an HD Map", IEEE IV 2019
- [8] Mohammad Aldibaja1, Ryo Yanase1, Tae Hyon Kim1, Akisue Kuramoto2, Keisuke Yoneda1, Noaki Suganuma, "Accurate Elevation Maps based Graph-Slam Framework for Autonomous Driving", IEEE IV 2019
- [9] Junichi Meguro, Takuya Arakawa, Syunsuke Mizutani and Aoki Takanose, "Low-cost Lane-level positioning in Urban Area Using Optimized Long Time Series GNSS and IMU Data", IEEE ITSC,2018
- [10] P.J.G. Teunissen, "The least-squares ambiguity decorrelation adjustment: a method for fast GPS integer ambiguity estimation", Journal of Geodesy (1995) 70:65-82.
- [11] Ren Kikuchi, Nobuaki Kubo, "Reliability Estimation for RTK-GNSS/IMU/Vehicle Speed Sensors in Urban Environment", IS-GNSS 2015
- [12] Nobuaki Kubo, Yize Zhang, Daisuke Hatta, "Integration of GNSS-PPP and IMU/SPEED Sensors in Urban Areas", ION 2019
- [13] Jan Sanromà Sánchez, et al, "Use of a FishEye Camera for GNSS NLOS Exclusion and Characterization in Urban Environments" ION2016
- [14] Yanlei Gu, et al, "SLAM with 3Dimensional-GNSS" IEEE/ION Position 2016
- [15] Motoki Higuchi and Nobuaki Kubo, "Achievement of Continuous Decimeter-Level Accuracy Using Low-Cost Single-Frequency Receivers in Urban Enviroments" MGA2016
- [16] Natsuka Shimizu, Kazuki Kusama, Taro Suzuki and Yoshiharu Amano, "Improving Accuracy of Single-Frequency RTK-GNSS using Satellite Selection and Doppler Frequency", IAIN, 2018.
- [17] Zhong,Xionghu, Ramtin,Rabiee, Yongsheng,Yan and Wee,Peng,Ta, "A particle filter for vehicle tracking with lane level accuracy under GNSS-denied environments" IEEE ITSC,2017
- [18] Gianluca.Falco, Marco.Pini, Gianluca.Marucco, "Loose and Tight GNSSINS Integrations_Comparison of Performance Assessed in Real Urban Scenarios," Sensors 2017,17,255, 2017
- [19] Xiaoli Meng, Heng Wang, and Bingbing Liu "A Robust Vehicle Localization Approach Based on GNSS/IMU/DMI/LiDAR Sensor Fusion for Autonomous Vehicles" Sensors 2017,17,2140, 2017
- [20] Junichi Meguro, Taishi Murata, Junichi Takiguchi, Yoshiharu Amano, Takumi Hashidume "GPS Multipath Mitigation for Urban Area Using Omnidirectional Infrared Camera" , IEEE Transactions on Intelligent Transportation Systems, 2009
- [21] Li-Ta Hsu "GNSS multipath detection using a machine learning approach",Intelligent Transportation Systems (ITSC),2017 IEEE 20th International Conference on, (2017)
- [22] Kojiro Takeyama, Yoshiko Kojima, Eiji Teramoto "Trajectory Estimation Improvement Based on Time-series Constraint of GPS Doppler and INS in Urban Areas" ,Proc. of IEEE/ION PLANS 2012, 700/705,(2012)
- [23] Kanwar, Bharat, Singh, "Vehicle Sideslip Angle Estimation Based on Tire Model Adaptation",electronics 2019,8,199
- [24] Selmanj Donald, Matteo Corno, Giulio Panzani, Sergio M.Savaresi,"Vehicle sideslip estimation A kinematic based approach" Control Eng. Pract. 2017, 67, 1–12.